Global Minimum Mass for Aerobraking Tethers

Steven G. Tragesser* and James M. Longuski†
Purdue University, West Lafayette, Indiana 47907-1282
and
Jordi Puig-Suari‡
Arizona State University, Tempe, Arizona 85287-6101

Introduction

THE proposed system consists of an orbiter and a probe connected by a long, thin tether (see Fig. 1). When the spacecraft arrives at a planet, the probe travels through the atmosphere and aerodynamic forces provide the change in velocity required to capture the vehicle into orbit around the planet, thus eliminating the need for chemical rockets. During the maneuver, the orbiter remains outside the sensible atmosphere and requires no aerodynamic shielding. Near periapsis, large aerodynamic torques on the vehicle tend to spin the tether and plunge the orbiter into the atmosphere, but this effect can be eliminated by spinning the tether in the opposite direction during approach, as shown in Fig. 1.

There are two maneuver types for the tethered-aerobraking maneuver.[1] In the vertical dumbbell maneuver, the tether is closely aligned with the local vertical near periapsis, i.e., $\alpha_{\min} \approx 0$ in Fig. 1. The maximum tension for this maneuver occurs outside of the atmosphere and is primarily due to spin rate. The case of $\alpha_{\min}$ greater than zero is referred to as an inclined maneuver; it exhibits maximum tension during the atmospheric flythrough. Knowledge about the dynamics of these maneuvers permits us to bound certain variables in the following analysis.

In Ref. 1, the (local) optimum tether mass is found using an exterior penalty, direction set method.[2] This direct search technique has several drawbacks including computational intensiveness, sensitivity to the initial guess, convergence problems, and lack of feedback to the user if the algorithm does not converge. In this Note, a method is employed that alleviates these problems and shows that previously found local minima are globally optimal solutions.

Problem Formulation

In general, there are five parameters that govern the aerobraking maneuver and tether design for a given spacecraft and approach trajectory. Three pertain to the system initial conditions: tether orientation α_0, spin rate $\dot{\alpha}_0$, and target periapsis altitude r_{per}. (Here we note that α_0 and $\dot{\alpha}_0$ can be specified at any point in the trajectory before atmospheric entry.) The other two parameters are the physical characteristics of the tether: length l and (uniform) diameter d. Constraints must be included in the formulation to guarantee that the resulting optimum maneuver is acceptable. First, the final eccentricity (after aerobraking) e_f must be equal to the eccentricity of the target orbit e_c. Next, the maximum force on the tether during the maneuver $F_{\max}$ cannot exceed the ultimate strength σ times the cross-sectional area of the tether A. Also, an inequality constraint is introduced so that the minimum altitude of the orbiter minus the minimum altitude of the probe (known as the orbiter's clearance), Δh, is greater than (or equal to) a set minimum, Δh_c. This ensures that the aerodynamic forces at the orbiter are insignificant. Finally, we require the minimum tension on the tether $T_{\min}$ to be nonnegative because compressive forces (negative tension) could cause severe bending in actual application. Mathematically the optimization problem of finding the maneuver with the minimum tether mass m can be written as follows.

Minimize

$$m(\bar{x}), \qquad \bar{x} \equiv \{\alpha_0, \dot{\alpha}_0, r_{\text{per}}, d, l\}^T$$

subject to

$$\begin{aligned} e_f - e_c = 0, \qquad & F_{\max} - \sigma A = 0 \\ \Delta h - \Delta h_c \geq 0, \qquad & T_{\min} \geq 0 \end{aligned} \tag{1}$$

The solution can be obtained using a number of numerical optimization procedures. Here we present a simple technique that is well suited for the problem under consideration.

Solution via Mapping Techniques

A simple way to verify a local minimum (or maximum) is to evaluate the objective function at neighboring points and determine whether it is always higher (or lower) at these points than at the candidate point. By expanding the region in the state space in which the objective function is evaluated, a map is made that can be used to search for local minima rather than verify a proposed solution. If the states of the problem are bounded, then the objective function can be completely characterized. This requires infinitely many points, but if the objective function is (piecewise) smooth, a finite number of points can be used to approximate the function.

Characterizing the objective function for the five state variables of Eqs. (1) would require an unreasonably large number of function evaluations. Furthermore, the objective function cannot be graphically depicted for a five-dimensional problem. To remedy these difficulties, the dimension of the state space is reduced using the equations of constraint. We set the inequality constraint for clearance identically equal to zero. (The results from Ref. 1 all achieved the minimum required clearance even though the constraint was enforced through an inequality. This seems physically reasonable because the tether can be made shorter to reduce the mass if excess clearance is obtained.) Then the eccentricity, tether strength, and clearance constraints of Eqs. (1) can be solved simultaneously to specify values for three of the parameters in $\bar{x}$, thereby reducing the number of free parameters to two. This allows the objective function to be completely characterized in two dimensions, with fewer points.

From experience, the process is quite robust if we choose to solve the constraint equations for r_{per}, d, and l. Then α_0 and $\dot{\alpha}_0$ can be varied over some range, and the value of m can be calculated at each point. After choosing the values of α_0 and $\dot{\alpha}_0$, we find the solution for the required tether mass by simultaneously solving

$$\begin{aligned} f_1(\tilde{x}) = e_f - e_c = 0, \qquad & f_2(\tilde{x}) = \Delta h - \Delta h_c = 0 \\ f_3(\tilde{x}) = F_{\max} - \sigma A = 0 & \end{aligned} \tag{2}$$

where $\tilde{x} \equiv [r_{\text{per}}, d, l]^T$. This is accomplished using a modified Powell hybrid method,[3] which is a variation of Newton's method. By repeating this process at many points, we obtain contours of the tether mass required for some subspace of α_0 and $\dot{\alpha}_0$.

Numerical Results

In Ref. 4, an analytic characterization of the optimal-mass tether problem proves that the atmosphere-bearing planets of the solar

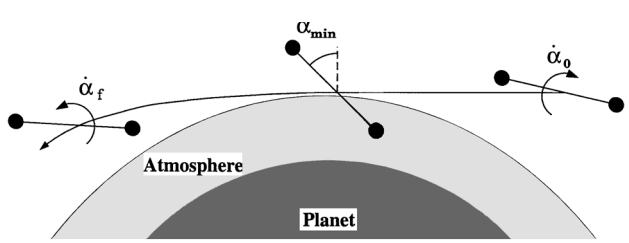

Fig. 1 Aerobraking maneuver.

Received Sept. 12, 1996; revision received Aug. 1, 1997; accepted for publication Aug. 4, 1997.

*Ph.D. Candidate, School of Aeronautics and Astronautics. Member AIAA.
†Associate Professor, School of Aeronautics and Astronautics. Associate Fellow AIAA.
‡Assistant Professor, Department of Mechanical and Aerospace Engineering. Member AIAA.

system can be categorized (by a particular scaling parameter) into two distinct groups, the terrestrial planets and the gas giants (where the satellite Titan turns out to be a gas giant). Within each group, the behavior of the optimal maneuver is very similar for a given ΔV. Accordingly, we now apply the mapping technique to one representative from each group, namely, Mars and Jupiter.

The case of aerocapture at Mars is investigated for capture into a nearly parabolic orbit ($e_f = 0.9999$) from a Hohmann transfer from Earth, using a Hercules AS4 graphite tether. Figure 2 shows the tether mass contours of aerocapture maneuvers that satisfy Eqs. (2). The α_0 and $\dot{\alpha}_0$ shown are for simulations where the initial altitude of the spacecraft center of mass is 256 km, which is well outside the sensible atmosphere. The orbiter and probe masses are each 1000 kg. A grid resolution of 61×51 (3111 data points) is used to generate the plot. Note that every point on the plot represents the tether mass required for the initial conditions indicated by the coordinates of the point (α_0, $\dot{\alpha}_0$). For example, if we choose an initial orientation of 0 deg and an initial spin rate of -0.0251 rad/s, then solving Eqs. (2) yields

$$r_{\text{per}} = 88.3\,\text{km}, \qquad l = 18.3\,\text{km}, \qquad d = 1.7\,\text{mm} \quad (3)$$

This length and diameter correspond to a tether mass of 75.0 kg, which corresponds to the value of the contour at 0 deg, -0.0251 rad/s in Fig. 2.

The initial orientation and spin rate are ideal variables for the two-dimensional search because they are both bounded for this problem. Because the tether orientation repeats itself every 360 deg, Fig. 2 includes all possible variations in α_0. (Notice how the plot matches exactly at $\alpha_0 = -180$ and 180 deg.) To bound $\dot{\alpha}_0$, we recall that the maximum tension of the vertical dumbbell maneuver is due to the exoatmospheric spin rate of the system. Thus, maneuvers with an initial spin rate greater (in magnitude) than the vertical dumbbell spin rate always have a higher maximum force (and larger tether diameter) than the vertical dumbbell. Therefore, the optimal solution must be located in the region where the magnitude of $\dot{\alpha}_0$ is less than that of the vertical dumbbell maneuver. In this example the vertical dumbbell maneuver has an $\dot{\alpha}_0$ of -0.0377 rad/s (and is indicated by an $\times$ in Fig. 2), and so the optimal solution must lie in the range $-0.0377 \leq \dot{\alpha}_0 \leq 0.0377$ rad/s. The positive range of $\dot{\alpha}_0$ was investigated but it is excluded from Fig. 2 for clarity. (Positive values correspond to spinning in the same direction as the orbital motion, opposite to the $\dot{\alpha}_0$ shown in Fig. 1, and are intuitively suboptimal.)

Within the search region of Fig. 2, there are combinations of α_0 and $\dot{\alpha}_0$ for which the altitude of the orbiter is lower than the altitude of the probe near periapsis. Because of this upside-down orientation, no tether length achieves the required clearance and, therefore, no solution is possible. These no-solution regions are shaded in Fig. 2 with dark gray and cannot contain the optimum.

When solving Eqs. (2), we ignore the constraint for $T_{\min}$ as given in Eqs. (1). Thus, maneuvers with compressive forces are present in the contours of Fig. 2. To exclude these areas from the search, any maneuvers containing compression are shaded in Fig. 2 with light gray. The boundary between the regions of no solution and compression is fairly irregular and probably not entirely accurate in certain areas due to numerical sensitivity. However, because this inaccuracy occurs in a region where the maneuvers already violate the compression constraint, more effort was not spent on improving this portion of the map.

Now that the search variables are bounded and the unacceptable maneuvers are eliminated, the global minimum tether mass is obtained simply by a visual inspection of the mass contours. In Fig. 2, there are closed elliptical contours in the center of the plot with values of 75 and 90 kg. Near the center of these contours is a local minimum mass of 65.7 kg. Further refinement of this solution with a map of the immediate vicinity (not shown) yields a tether mass of 64.9 kg. A quick survey of the rest of Fig. 2 reveals no other minima that satisfy the constraints, indicating that this solution is the global minimum.

The computational time needed to generate the 3111 data points of Fig. 2 [each requiring several trajectory simulations to solve Eqs. (2)] is comparable to the computational intensiveness of the direct search method in Ref. 1. In practice, however, a much lower resolution can be used in the mapping technique to visually determine the approximate region where the optimum is located. Then successive enlargements (with relatively few data points) can be used to improve the accuracy of the solution. This is typically a faster and more robust process than the local search technique.

The reason for difficulties with the direct search method in Ref. 1 can be deduced from Fig. 2. There are local minima present in the compression region (near the no-solution areas) toward which the direct search and descent methods are drawn because the numerical search is initially driven by the unconstrained problem. (Note that an exterior penalty method is used in Ref. 1.) This region is numerically very sensitive, however, and the conventional search algorithm would sometimes fail to converge.

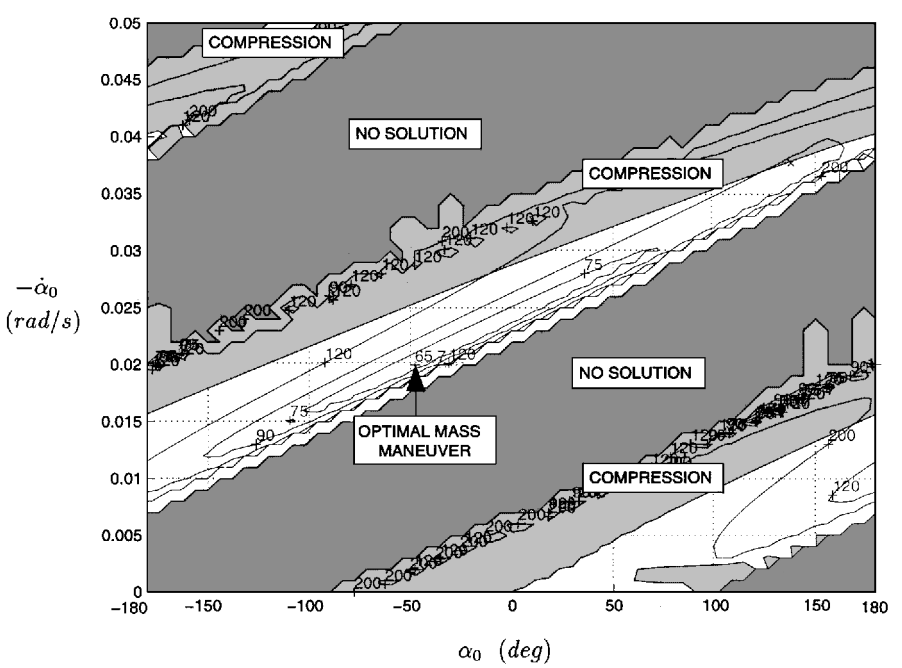

Fig. 2 Mass map and compression constraint at Mars (e_f = 0.9999); contours are in kilograms.

Table 1 Optimal mass aerobraking tethers using mapping technique

Values	Venus	Earth	Mars	Jupiter	Saturn	Uranus	Neptune	Titan
ΔV, km/s	0.35	0.39	0.67	0.27	0.41	0.50	0.34	1.31
Tether mass, kg	25.7	30.1	64.9	18.8	44.4	67.2	32.5	279
Length, km	12.2	10.5	19.3	36.1	54.4	72.7	72.7	108
Diameter, mm	1.22	1.42	1.54	0.608	0.760	0.809	0.562	1.35
Maximum force, N	4210	5720	6730	1040	1630	1850	894	5160
Minimum α, deg	27.8	31.2	40.4	−0.28	−0.21	−0.57	−1.07	38.1
Maneuver type[a]	I	I	I	V	V	V	V	I

[a]I is inclined maneuver, and V is vertical dumbbell maneuver.

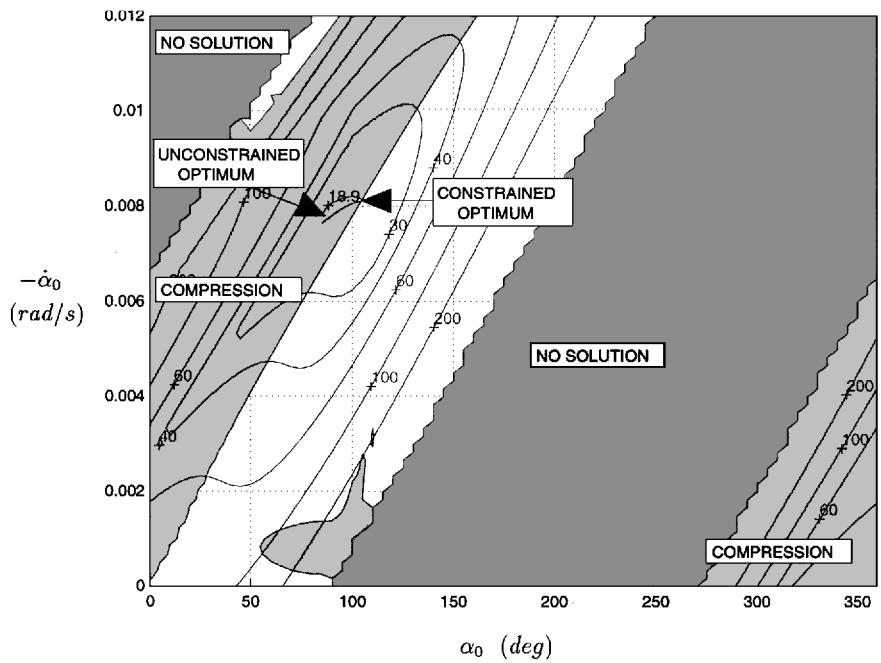

Fig. 3 Mass map and compression constraint at Jupiter (e_f = 0.9999); contours are in kilograms.

The mapping technique also allows for insight to be gained regarding the nature of the optimal solution. In Fig. 2, we see that the mass contours are smooth near the optimum and that the solution is far from areas where the constraints are not satisfied (in regions of no solution or compression). This illustrates the attractiveness of the inclined maneuver for possible guidance and control applications inasmuch as small perturbations in the initial conditions are not likely to be catastrophic.

The mass map is similar for the other terrestrial planets (Venus and Earth). In the same manner as just described, we can bound the area that must contain the optimum solution. Within this region we find that there is a unique minimum that turns out to be an inclined maneuver. We can then conclude that this is the global minimum. The results are shown in Table 1.

The behavior for the cases of aerocapture at the gas giants is very different from the optimal inclined maneuvers at the terrestrial planets. To illustrate, we analyze aerocapture at Jupiter (for $e_f = 0.9999$). The contour plot representing the solution for Eqs. (2) is shown in Fig. 3, where the initial orientation and spin rate correspond to an initial altitude of 1220 km.

For this case, the only (unconstrained) local minimum mass is located in the region of compression. Once we enforce the compression constraint, however, the best answer is found at the edge of the constraint with a value of 18.9 kg. Thus, the minimum tension during atmospheric flythrough is equal to zero, which is characteristic of the vertical dumbbell maneuver. This constrained optimum is the global minimum tether mass for aerocapture at Jupiter.

The optimum-mass tethers for the other gas giants (Saturn, Uranus, Neptune, and Titan) are given in Table 1. Except for Titan, the unconstrained minimum in each of these cases contains compressive forces just as it did at Jupiter. Consequently, the (constrained) solution is a vertical dumbbell (bordering the region of compression). At Titan, the mass map is more closely related to the terrestrial planets, and it yields an inclined solution for the optimum.

Both the maneuver type and tether mass for all of the cases given in Table 1 closely match the results from Ref. 1. The results here, however, were found with less difficulty and greater precision.

Conclusion

The local minimum mass solutions obtained previously for the aerobraking tether appear to be global optima. An exhaustive search reveals no new type of tether aerobraking maneuver; therefore, the optima consist of vertical dumbbell maneuvers and inclined maneuvers.

The mapping technique is a direct method that does not require an initial guess for the location of the optimum, retains information about other maneuvers, and is very robust.

References

[1]Longuski, J. M., Puig-Suari, J., Tsiotras, P., and Tragesser, S. G., "Optimal Mass for Aerobraking Tethers," *Acta Astronautica*, Vol. 35, No. 8, 1995, pp. 489–500.

[2]Rao, S. S., "Nonlinear Programming II: Unconstrained Optimization," *Optimization: Theory and Applications*, Wiley, New York, 1984, pp. 269–283.

[3]More, J., Garbow, B., and Hillstrom, K., "User Guide for MINIPACK-1," Argonne National Labs., ANL-80-74, Argonne, IL, March 1980.

[4]Tragesser, S. G., Longuski, J. M., and Puig-Suari, J., "A General Approach to Aerobraking Tether Design," American Astronautical Society, AAS Paper 95-353, Halifax, NS, Canada, Aug. 1995.